

SUPPORTING INFORMATION

Effect on the coordination number over the slow relaxation of the magnetization in a series of Erbium(III) complexes based on halogenated ligands

Jérôme Long,^{*a,b} Dmitry M. Lyubov,^{c,d} Alexander A. Kissel',^d Ilia A. Gogolev,^d Andrey A. Tyutyunov,^d Yulia V. Nelyubina,^d Fabrice Salles,^a Yannick Guari,^a Anton V. Cherkasov,^c Joulia Larionova^a and Alexander A. Trifonov^{*c,d}

^a ICGM, Univ. Montpellier, CNRS, ENSCM, Montpellier, France. E-mail: jerome.long@umontpellier.fr

^b Institut Universitaire de France (IUF), 1 rue Descartes, 75231 Paris Cedex 05, France.

^c Institute of Organometallic Chemistry of Russian Academy of Sciences, 49 Tropinina str., GSP-445, 603950, Nizhny Novgorod, Russia. E-mail: trif@iomc.ras.ru

^d A.N. Nesmeyanov Institute of Organoelement Compounds of Russian Academy of Sciences, 28 Vavilova str., 119334, Moscow, Russia.

TABLE OF CONTENTS

Figure S1: Perspective view of the crystal packing for 1- 5 along some crystallographic axes. Hydrogen atoms have been omitted for clarity.....	4
Figure S2: Temperature dependence of χT for 1 - 5. Samples 1, 4 and 5 were measured under an applied magnetic field of 1000 Oe, while the data for samples 2 and 3 were measured under a 10 kOe to decrease the contribution from temperature independent paramagnetism. Inset: field dependence of the magnetization at 1.8 K for 1-5. The red solid lines correspond to the calculated curves from the <i>ab initio</i> calculations.....	5
Figure S3: Frequency dependence of χ' and χ'' for 1–5 for different temperatures performed under various dc fields.....	6
Figure S4: Cole-Cole (Argand) plots obtained using the ac susceptibility data for 5 (0 Oe). The solid lines correspond to the best fit obtained with a generalized Debye model.....	7
Figure S5: Frequency dependence of χ' and χ'' for different temperatures performed under a 1500 (1) or 1000 Oe (5) dc field.	7
Figure S6: Cole-Cole (Argand) plots obtained using the ac susceptibility data for 1 (1500 Oe) and 5 (1000 Oe). The solid lines correspond to the best fit obtained with a generalized Debye model.....	8
Figure S7: Anisotropic axes (purple) for the KD ground state obtained from the <i>ab initio</i> calculations.....	9
Table S1: Crystal data and structure refinement details for 1-5.	10
Table S2: SHAPE{Casanova, 2005 #267} analysis for 1-5.	11
Table S3: Fitting of the Cole-Cole plots with a generalized Debye model under a 0 Oe dc field for 5.	11
Table S4: Fitting of the Cole-Cole plots with a generalized Debye model under a 1500 Oe dc field for 1.....	12
Table S5: Fitting of the Cole-Cole plots with a generalized Debye model under a 1000 Oe dc field for 5.....	12
Table S6: <i>Ab initio</i> calculated energies, <i>g</i> -tensor main values of the ground doublet and the n^{th} KD doublet for the ground multiplet $J = 15/2$ obtained for 1.	12
Table S7: <i>Ab initio</i> calculated energies, <i>g</i> -tensor main values of the ground doublet and the n^{th} KD doublet for the ground multiplet $J = 15/2$ obtained for 2.	13
Table S8: <i>Ab initio</i> calculated energies, <i>g</i> -tensor main values of the ground doublet and the n^{th} KD doublet for the ground multiplet $J = 15/2$ obtained for 3.	13
Table S9: <i>Ab initio</i> calculated energies, <i>g</i> -tensor main values of the ground doublet and the n^{th} KD doublet for the ground multiplet $J = 15/2$ obtained for 4.	13
Table S10: <i>Ab initio</i> calculated energies, <i>g</i> -tensor main values of the ground doublet and the n^{th} KD doublet for the ground multiplet $J = 15/2$ obtained for 5.	14
Table S11: Weight of individual crystal-field parameters on the crystal-field splitting obtained by <i>Ab initio</i> for 5a. Only values larger than 1% are given.....	14
Table S12: Weight of individual crystal-field parameters on the crystal-field splitting obtained by <i>Ab initio</i> for 5b. Only values larger than 1% are given.....	15

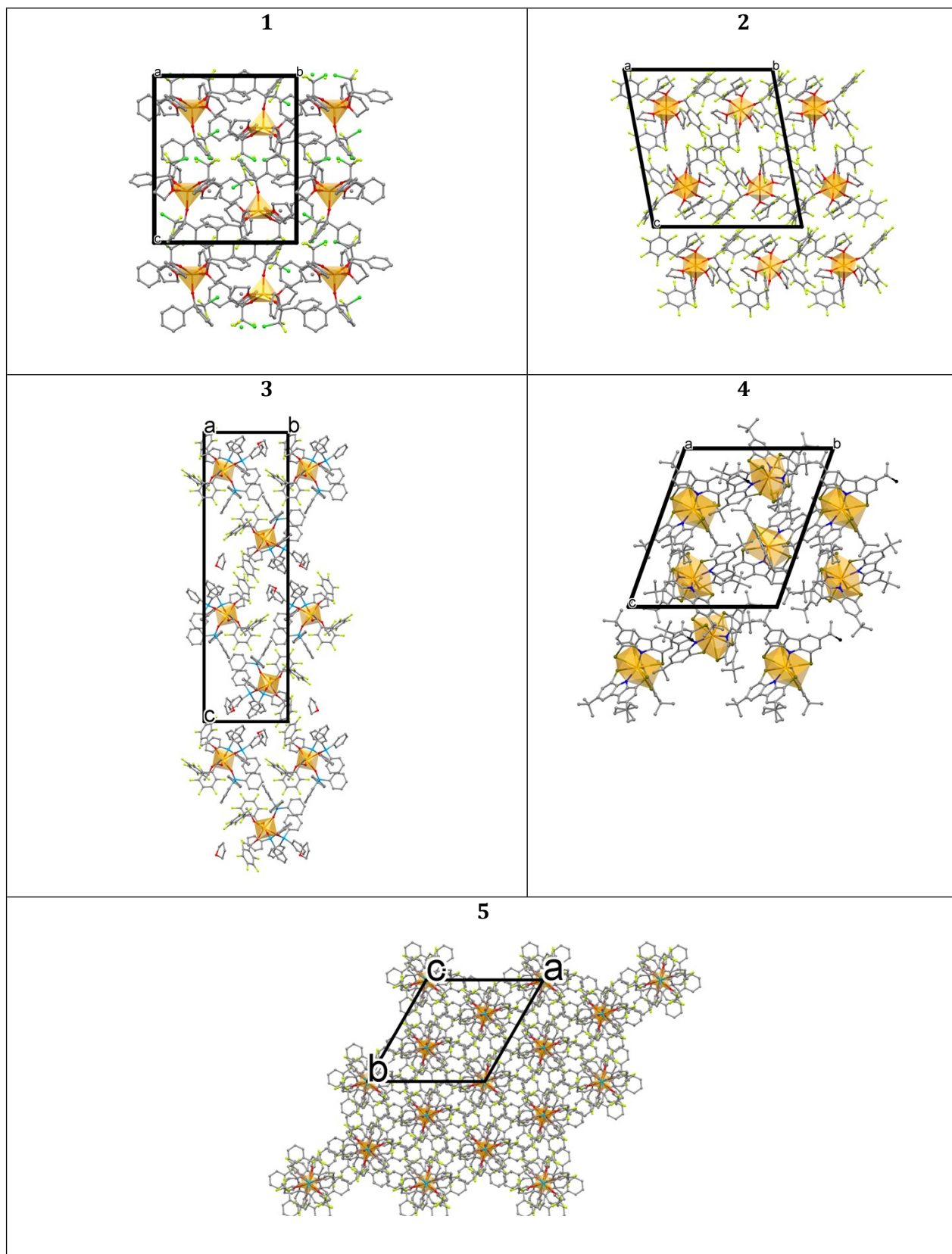


Figure S1: Perspective view of the crystal packing for 1- 5 along some crystallographic axes. Hydrogen atoms have been omitted for clarity.

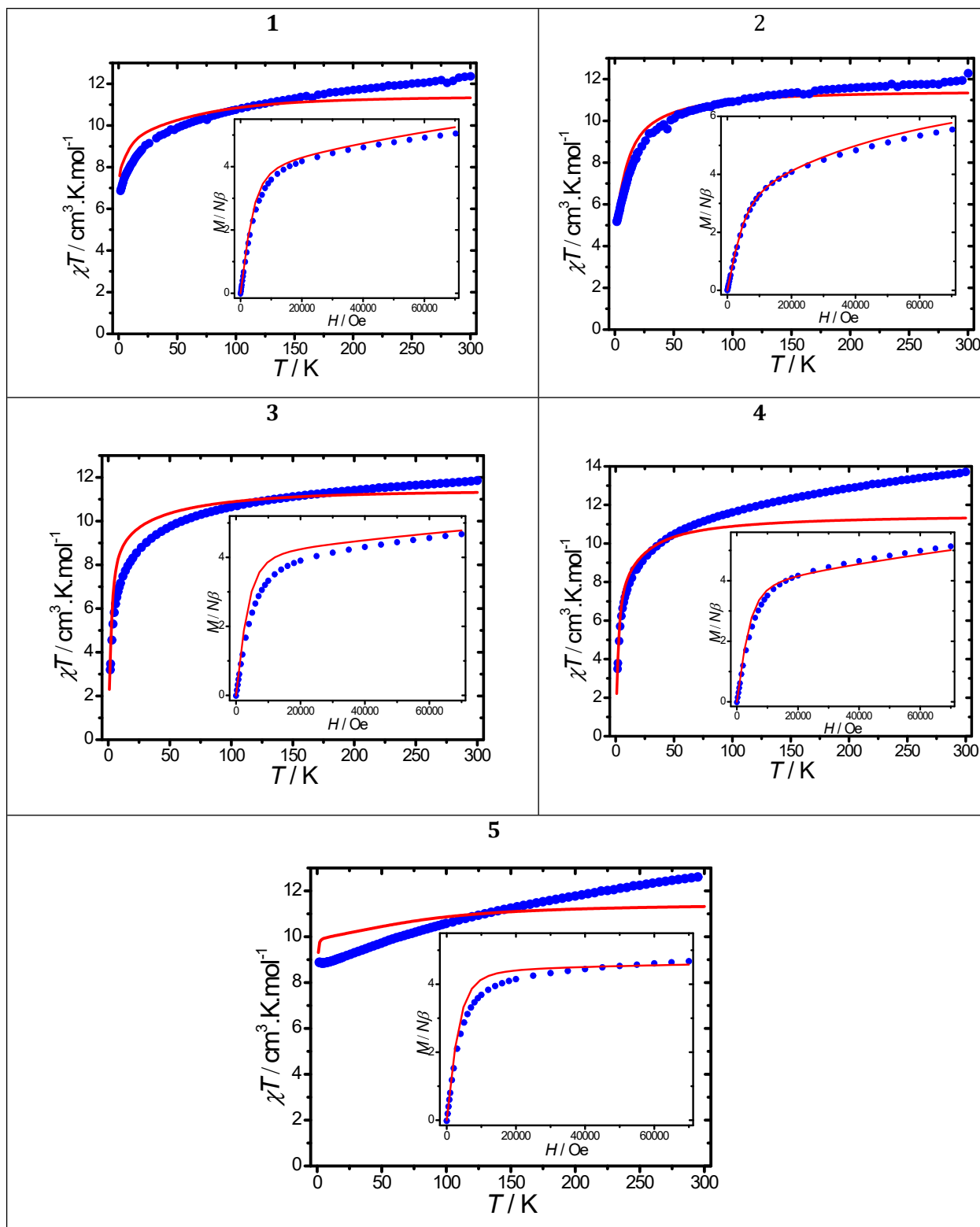


Figure S2: Temperature dependence of χT for 1 - 5. Samples 1, 2 and 5 were measured under an applied magnetic field of 1000 Oe, while the data for samples 3 and 4 were measured under a 10 kOe to decrease the contribution from temperature independent paramagnetism. Inset: field dependence of the magnetization at 1.8 K for 1-5. The red solid lines correspond to the calculated curves from the *ab initio* calculations.

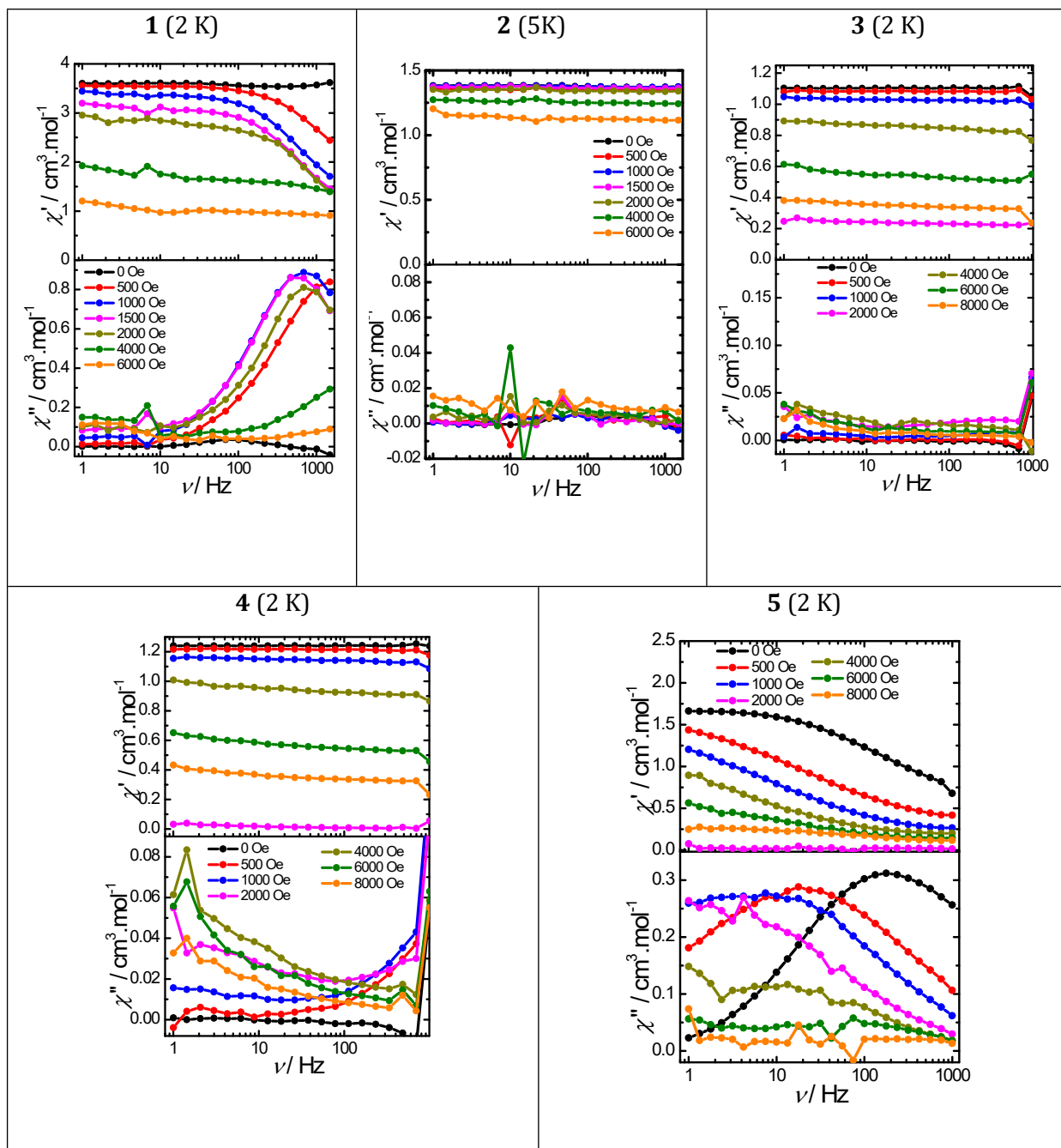


Figure S3: Frequency dependence of χ' and χ'' for 1–5 for different temperatures performed under various dc fields.

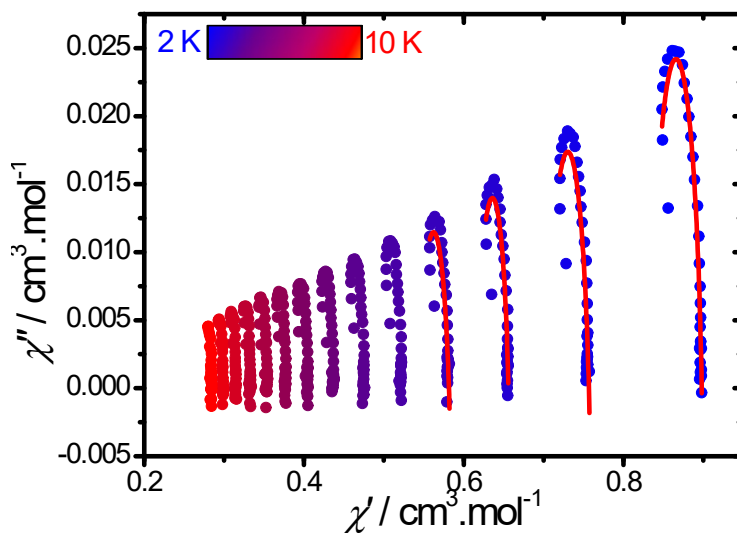


Figure S4: Cole-Cole (Argand) plots obtained using the ac susceptibility data for **5** (0 Oe). The solid lines correspond to the best fit obtained with a generalized Debye model.

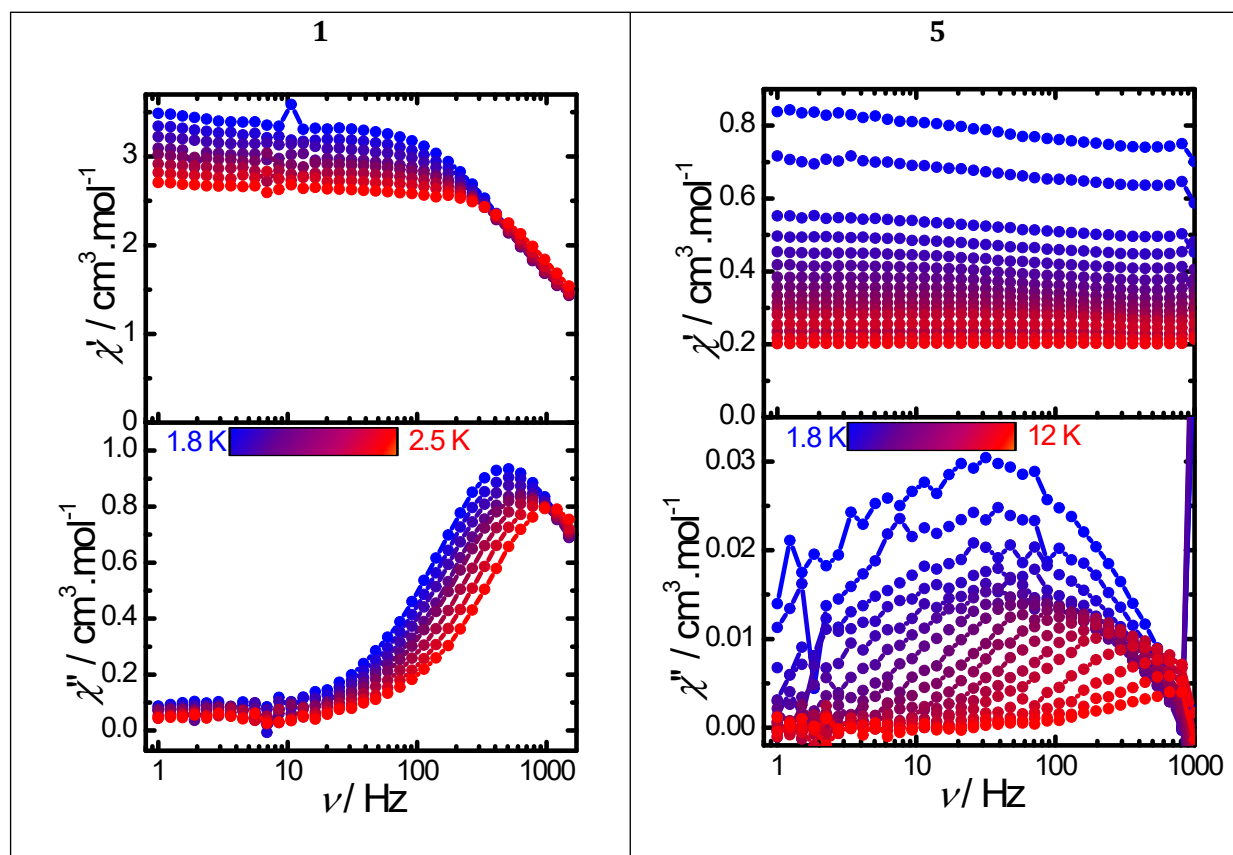


Figure S5: Frequency dependence of χ' and χ'' for different temperatures performed under a 1500 (1) or 1000 Oe (5) dc field.

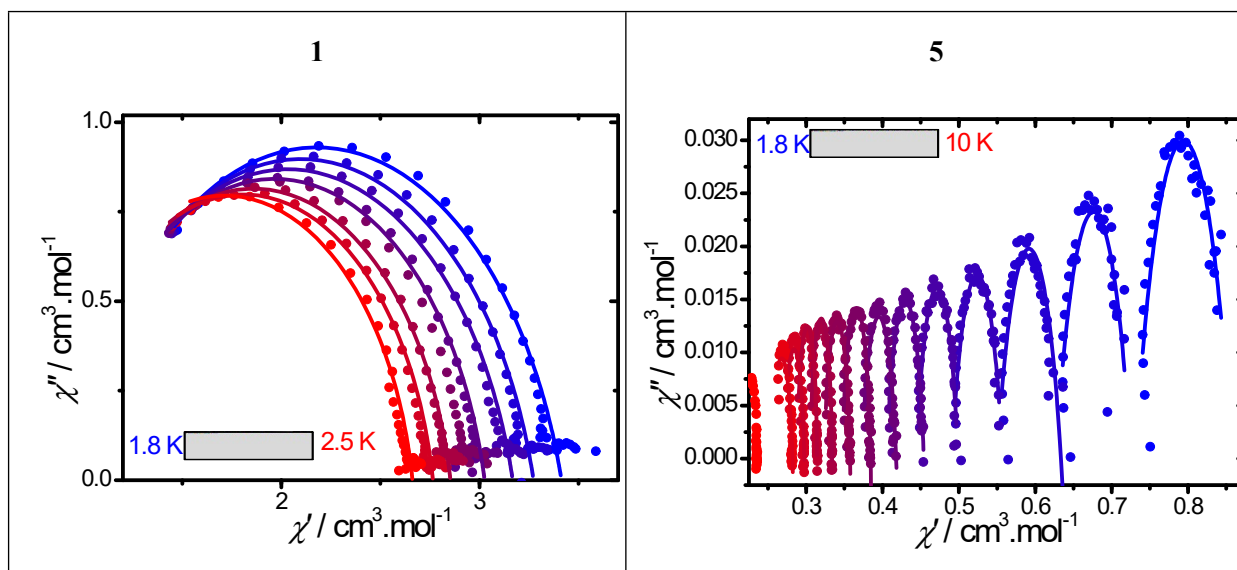


Figure S6: Cole-Cole (Argand) plots obtained using the ac susceptibility data for 1 (1500 Oe) and 5 (1000 Oe). The solid lines correspond to the best fit obtained with a generalized Debye model.

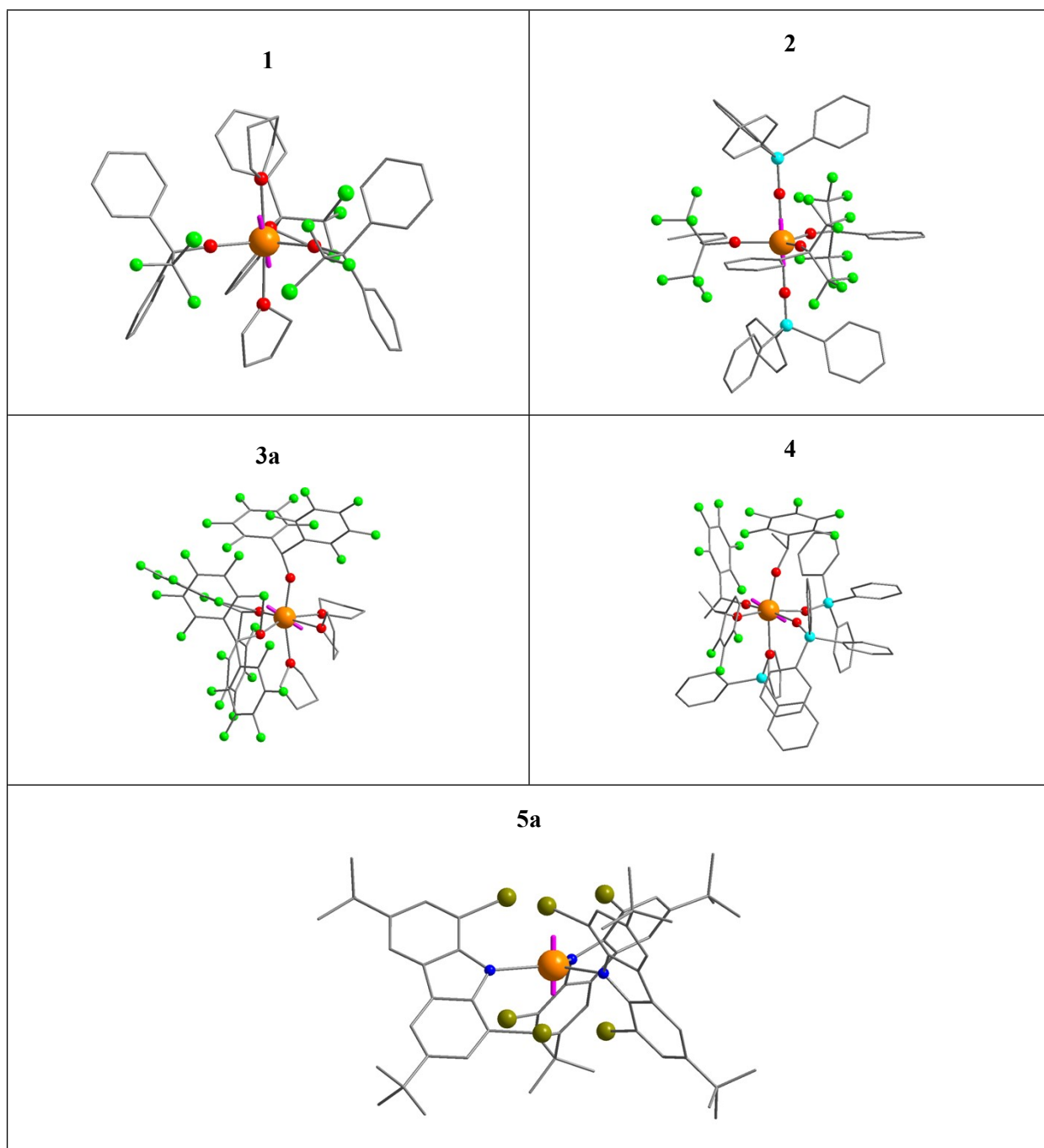


Figure S7: Anisotropic axes (purple) for the KD ground state obtained from the *ab initio* calculations.

Table S1: Crystal data and structure refinement details for **1-5**.

	1	2	3	4	5
Formula	C ₅₀ H ₄₆ Cl ₃ ErF ₆ O ₅	C ₆₃ H ₄₅ ErF ₁₈ O ₅ P ₂	C ₅₁ H ₂₇ ErF ₃₀ O ₆	C ₇₈ H ₅₇ ErF ₁₅ O ₆ P ₃ , C ₄ H ₈ O	C ₆₀ H ₆₆ Br ₆ ErN ₃
<i>M</i>	1114.48	1453.56	1472.98	1707.51	1475.87
<i>T</i> , K	100	100	100	100	100
Crystal system	Monoclinic	Trigonal	Triclinic	Monoclinic	Triclinic
Space group	<i>P</i> 2 ₁ / <i>n</i>	<i>R</i> -3	<i>P</i> -1	<i>P</i> 2 ₁ / <i>n</i>	<i>P</i> -1
<i>Z</i> (<i>Z'</i>)	4 (1)	6 (1/3)	4 (2)	4 (1)	2 (1)
<i>a</i> , Å	15.7102(3)	18.885(12)	12.326(4)	12.3834(3)	16.6814(8)
<i>b</i> , Å	15.8031(3)	18.885(12)	19.924(7)	13.1486(3)	18.4271(9)
<i>c</i> , Å	18.5149(3)	28.24(2)	22.015(8)	45.3406(12)	20.8840(10)
<i>α</i> , deg	90	90	79.645(8)	90	106.146(2)
<i>β</i> , deg	92.7490(10)	90	76.492(8)	93.0260(10)	102.283(2)
<i>γ</i> , deg	90	120	89.899(8)	90	101.556(2)
<i>V</i> , Å ³	4591.40(14)	8722(13)	5167(3)	7372.3(3)	5790.3(5)
<i>d</i> _{calcd} , g·cm ⁻³	1.612	1.660	1.894	1.538	1.693
<i>μ</i> , mm ⁻¹	20.74	16.07	17.84	12.97	5.629
<i>F</i> ₀₀₀	2236	4339	2876	3444	2900
<i>θ</i> _{max} , deg	54	50	50	50	25.03
Number of measured refl.	52446	41894	45934	70715	65945
Number of independent refl. (<i>R</i> _{int})	10022	3415	18185	13600	20392 (0.0702)
Observed refl. [<i>I</i> > 2σ(<i>I</i>)]	8557	1610	12301	12267	14292
Parameters	603	257	1586	1005	1330
<i>R</i> ₁ and <i>wR</i> ₂ [<i>F</i> ² > 2σ(<i>F</i> ²)]	0.0256	0.1080	0.1258	0.0722	0.0531, 0.0924
<i>R</i> ₁ and <i>wR</i> ₂ (all data)	0.0586	0.3017	0.3648	0.1482	0.0898, 0.1039
<i>S</i> (<i>F</i> ²)	1.013	1.055	1.258	1.230	1.054
Residual electron density (<i>d</i> _{max} / <i>d</i> _{min}), e·Å ⁻³	1.160/-0.563	1.672/-0.773	6.435/-1.876	3.234/-5.360	1.91 / -1.51

Table S2: SHAPE¹ analysis for 1-5.

		PP	VOC	TBPY	SPY	JTBPY
1		33.378	4.912	0.750	3.954	1.452
2		36.962	7.225	0.171	5.553	2.072
PP: Pentagon vOC: Vacant octahedron TBPY: Trigonal bipyramid SPY: Spherical square pyramid JTBPY: Johnson trigonal bipyramid J12						
		HP	PPY	OC	TPR	JPPY
3	a	32.015	26.678	0.618	14.943	30.204
	b	31.859	26.974	0.608	15.682	30.496
4		33.185	29.265	0.232	16.279	32.916
HP: Hexagon PPY: Pentagonal Pyramid OC: Octahedron TPR: Trigonal Prism JPPY: Johnson Pentagonal Pyramid						
		TP	vT	fvOC	mvOC	
5	a	0.156	2.587	10.157	8.525	
	b	0.110	2.830	10.644	8.144	
TP: Trigonal vT: Vacant tetrahedron fvOC: fac-Trivacant octahedron mvOC: mer-Trivacant octahedron						

Table S3: Fitting of the Cole-Cole plots with a generalized Debye model under a 0 Oe dc field for 5.

<i>T</i> (K)	χ_s (cm ³ . mol ⁻¹)	χ_T (cm ³ . mol ⁻¹)	α
1.8	0.83961	0.89208	0.218
2.28	0.71152	0.7491	0.348
2.75	0.62074	0.65119	0.286
3.23	0.55042	0.57406	0.460

Table S4: Fitting of the Cole-Cole plots with a generalized Debye model under a 1500 Oe dc field for **1**.

T (K)	χ_S (cm ³ . mol ⁻¹)	χ_T (cm ³ . mol ⁻¹)	α
1.80007	0.94484	3.41428	0.17811
1.90036	0.92478	3.27336	0.1692
2.00004	0.89931	3.1682	0.16787
2.10008	0.90788	3.02616	0.1449
2.29985	0.86774	2.85356	0.1252
2.39974	0.85137	2.76501	0.11461
2.49973	0.76688	2.66186	0.11092

Table S5: Fitting of the Cole-Cole plots with a generalized Debye model under a 1000 Oe dc field for **5**.

T (K)	χ_S (cm ³ . mol ⁻¹)	χ_T (cm ³ . mol ⁻¹)	α
1.8	0.78533	0.80254	0.89392
2.31	0.66894	0.68337	0.88514
2.83	0.5872	0.59646	0.91402
3.35	0.50998	0.53783	0.65642
3.86	0.455	0.48804	0.46633
4.38	0.41408	0.44538	0.42508
4.9	0.38139	0.40888	0.46549
5.41	0.35039	0.3811	0.20038
5.93	0.32655	0.35451	0.20325
6.45	0.30625	0.3333	0.04604
7	0.28899	0.31402	0.00779
7.48	0.27299	0.29518	0.19483
8	0.25761	0.2781	0.33473

Table S6: *Ab initio* calculated energies, g-tensor main values of the nth KD doublet for the ground multiplet $J = 15/2$ obtained for **1**.

KD	Energy (cm ⁻¹)	g_x	g_y	g_z	Wavefunction (only component with > 10 % are given)
1	0.00	0.36194471	0.59827551	15.76201956	52.5% $\pm 13/2$ >; 32.9% $\pm 15/2$ >
2	26.685	0.32466487	0.55290517	13.63356657	36.0% $\pm 9/2$ >; 34.6% $\pm 11/2$ >; 12.2% $\pm 7/2$ >; 10.2% $\pm 13/2$ >
3	116.298	2.74126368	3.71106997	9.30630729	38.8% $\pm 11/2$ >; 25.1% $\pm 7/2$ >; 10.9% $\pm 9/2$ >; 10.1% $\pm 3/2$ >
4	174.853	8.52102702	6.58951045	2.48264088	25.5% $\pm 5/2$ >; 24.1% $\pm 9/2$ >; 18.4% $\pm 7/2$ >; 17.18% $\pm 1/2$ >;
5	207.456	0.78097429	1.48152853	15.60255568	28.1% $\pm 3/2$ >; 19.0% $\pm 5/2$ >; 17.8% $\pm 1/2$ >; 16.0% $\pm 7/2$ >; 14.9% $\pm 9/2$ >;
6	245.462	0.03125194	2.82254607	14.27971112	49.9% $\pm 15/2$ >; 24.0% $\pm 13/2$ >
7	252.577	0.66561281	3.50378641	11.83400606	21.2% $\pm 5/2$ >; 21.0% $\pm 3/2$ >; 14.1% $\pm 7/2$ >; 14.0% $\pm 15/2$ >
8	338.113	0.03156249	0.11098655	17.73860739	42.2% $\pm 1/2$ >; 29.1% $\pm 3/2$ >; 15.4% $\pm 7/2$ >

Table S7: *Ab initio* calculated energies, g-tensor main values of the nth KD doublet for the ground multiplet $J = 15/2$ obtained for **2**.

KD	Energy (cm ⁻¹)	g_x	g_y	g_z	Wavefunction (only component with > 10 % are given)
1	0.00	0.79758565	0.81299521	12.90155100	98.6% ±11/2>
2	17.462	0.75078663	0.75209747	15.4019330	99.1% ±13/2>
3	65.535	0.03902774	0.05941930	10.10499247	95.5% ±9/2>
4	118.378	7.52598206	7.48472464	4.91877105	75.8% ±7/2>; 23.7% ±5/2 >
5	153.680	10.08425816	8.44208269	0.84970268	93.6% ±1/2>
6	162.302	0.55084622	0.99451007	3.01525951	95.2% ±3/2>
7	170.627	7.96231982	7.49852299	2.26873026	72% ±5/2>; 23.7% 7±/2>;
8	330.693	0.00003599	0.00020951	17.92189517	99.9% ±15/2>

Table S8: *Ab initio* calculated energies, g-tensor main values of the nth KD doublet for the ground multiplet $J = 15/2$ obtained for **3**.

3a					
KD	Energy (cm ⁻¹)	g_x	g_y	g_z	Wavefunction (only component with > 10 % are given)
1	0.00	0.15936250	0.31019731	16.51981489	81.3% ±15/2>; 15.7% ±9/2>
2	55.498	0.62353324	0.84436626	13.4464878	69.4% ±13/2>; 22.9% ±7/2>
3	120.461	2.17843669	3.76615881	9.01800905	46.8% ±11/2>; 33.7% ±5/2>
4	165.184	0.00996387	4.39913270	10.92167487	41.6% ±3/2>; 37.2% ±1/2>
5	180.734	2.44785680	4.94520631	10.66668572	47.7% ±1/2>; 29.1% ±3/2>
6	283.934	0.09404577	0.68825241	16.48322742	29.1% ±5/2>; 20.3% ±9/2>; 16.3% ±3/2>; 14.4% ±7/2>; 11.4% ±11/2>;
7	332.401	0.09849091	2.39080804	13.00117483	28.1% ±11/2>; 16.6% ±5/2>; 14.0% ±9/2>
8	341.174	0.05204274	2.29318251	13.15470965	33.4% ±9/2>; 27.9% ±7/2>; 14.2% ±13/2>
3b					
KD	Energy (cm ⁻¹)	g_x	g_y	g_z	Wavefunction (only component with > 10 % are given)
1	0.00	0.14512192	0.31918615	16.48118915	81.0% ±15/2>; 14.7% ±9/2>
2	50.444	0.70970909	0.96179950	13.78607519	66.4% ±13/2>; 16.5% ±7/2>
3	120.368	1.82460497	2.94628488	9.60736636	45.9% ±11/2>; 22.6% ±5/2>; 15.7% ±7/2>
4	160.172	0.39086475	4.20097429	12.08423915	49.0% ±3/2>; 25.5% ±1/2>; 11.2% ±5/2>
5	181.138	2.62284623	5.61732347	9.08405140	60.2% ±1/2>; 11.1% ±3/2>; 10.6% ±5/2>
6	301.947	0.57005445	0.82285788	15.74600398	26.4% ±3/2>; 25.1% ±5/2>; 21.3% ±9/2>
7	339.452	0.26556833	1.24151654	16.48413235	32.4% ±7/2>; 15.6% ±1/2>; 15.1% ±9/2>; 13.5% ±5/2>; 12.1% ±13/2>;
8	367.690	0.11808566	0.25181705	17.44290560	28.3% ±9/2>; 22.4% ±7/2>; 18.2% ±11/2>; 11.8% ±13/2>; 11.7% ±3/2>;

Table S9: *Ab initio* calculated energies, g-tensor main values of the nth KD doublet for the ground multiplet $J = 15/2$ obtained for **4**.

KD	Energy (cm ⁻¹)	g_x	g_y	g_z	Wavefunction (only component with > 10 % are given)
1	0.00	0.46264204	1.00682194	15.46819953	70.8% ±15/2>; 14.6% ±7/2>
2	34.482	2.29606896	4.08856018	12.18589656	43.5% ±13/2>; 18.6% ±7/2>; 16.3% ±11/2>
3	72.163	0.04839228	1.59675796	14.73818601	40.6% ±1/2>; 32.1% ±3/2>; 14.5% ±5/2>
4	88.658	6.80581425	5.45879715	2.75997663	20.2% ±11/2>; 17.3% ±7/2>; 16.5% ±2/2>; 16.2% ±5/2>; 13.1% ±9/2>
5	128.277	1.46492288	1.87315280	11.93716450	35.3% ±1/2>; 21.1% ±3/2>; 15.5% ±5/2>
6	285.527	1.13996043	2.05331026	14.19567575	23.8% ±9/2>; 20.0% ±7/2> 15.2% ±11/2>; 11.9% ±13/2>; 11.7% ±3/2>; 10.1% ±5/2>
7	326.051	0.16847203	2.92759879	14.39351091	27.6% ±5/2>; 21.7% ±7/2>; 15.6% ±11/2>; 11.8% ±3/2>; 10.4% ±1/2>
8	359.189	0.05997224	0.95856972	16.67255039	28.0% ±9/2>; 22.6% ±11/2>; 21.6% ±13/2>; 11.9% ±7/2>

Table S10: *Ab initio* calculated energies, g-tensor main values of the nth KD doublet for the ground multiplet $J = 15/2$ obtained for **5**.

5a					
KD	Energy (cm ⁻¹)	g_x	g_y	g_z	Wavefunction (only component with > 10 % are given)
1	0.00	0.02529856	0.03726463	17.78194475	97.9% ±15/2>
2	171.549	1.15623517	5.22463722	10.19226168	44.6% ±9/2>; 22.4% ±13/2>; 11.1% ±7/2>
3	185.021	0.07910381	3.92043253	7.86254799	37.8% ±9/2>; 26.8% ±13/2>; 15.9% ±11/2>; 10.7% ±7/2>
4	195.549	1.02091528	2.61011850	9.75125540	61.7% ±11/2>; 21.5% ±13/2>; 10.5% ±5/2>
5	205.770	2.36186776	5.12317032	9.92125043	41.7% ±7/2>; 28.0% ±13/2>; 14.3% ±5/2>
6	370.647	8.75738481	6.19116984	2.40606448	69.0% ±5/2>; 23.4% ±7/2>
7	442.973	2.28963234	3.46661799	5.66178084	82.9% ±3/2>
8	509.824	0.71759192	4.32950223	13.74094096	83.9% ±1/2>
5b					
KD	Energy (cm ⁻¹)	g_x	g_y	g_z	Wavefunction (only component with > 10 % are given)
1	0.000	0.01020999	0.01655472	17.79970508	98.1% ±15/2>
2	179.856	8.84277516	6.01254454	0.19706720	77.3% ±9/2>
3	191.573	3.98546980	2.95495764	0.67307761	29.5% ±11/2>; 28.4% ±13/2>; 20.1% ±7/2>; 10.9% ±9/2>
4	203.827	1.52508654	2.62571140	8.01116051	55.2% ±11/2>; 29.1% ±7/2>
5	210.718	3.61381869	5.27619287	10.21368291	58.7% ±13/2>; 24.2% ±7/2>
6	377.757	8.72190425	5.84721757	2.74921564	72.4% ±5/2>; 20.9% ±7/2>
7	463.215	1.30507688	2.66293602	4.49909167	88.7% ±3/2>
8	530.747	0.90345492	6.30296829	12.23013262	88.6% ±1/2>

Table S11: Weight of individual crystal-field parameters on the crystal-field splitting obtained by *Ab initio* for **5a**. Only values larger than 1% are given.

k	q	B_k^q 5a	Weight in % 5a
2	0	-2.27E+00	28.9095836
6	-6	9.02E-05	19.5733841
6	0	-5.40E-05	11.7122942
6	-3	3.35E-05	7.2607183
4	0	1.89E-03	4.37074636
2	-2	-3.33E-01	4.25072347
4	-3	-1.31E-03	3.04205002
6	3	-1.27E-05	2.75024222
6	5	-1.14E-05	2.47999549
6	-2	-1.07E-05	2.31696919
4	3	9.13E-04	2.11253214
4	4	8.89E-04	2.05728315
6	4	-7.72E-06	1.67541902

Table S12: Weight of individual crystal-field parameters on the crystal-field splitting obtained by *Ab initio* for **5b**. Only values larger than 1% are given.

<i>k</i>	<i>q</i>	B_k^q 5b	Weight % 5b
2	0	-2.35E+00	29.0961027
6	-6	-8.73E-05	18.362576
6	0	-6.05E-05	12.715981
6	-3	-2.82E-05	5.92240496
6	3	-2.63E-05	5.53899602
4	0	2.19E-03	4.91077444
6	6	-2.02E-05	4.25245739
4	-3	1.37E-03	3.0626941
4	3	1.18E-03	2.65438539
4	4	-1.00E-03	2.2427206
2	-2	-1.49E-01	1.83966372
6	-2	-7.48E-06	1.57256301
2	2	-1.21E-01	1.49058188
4	-4	-4.53E-04	1.01482646

1 D. Casanova, M. Llunell, P. Alemany and S. Alvarez, *Chem. Eur. J.*, 2005, **11**, 1479-1494.